

Research Article

Cyanobacterial Biomass Pigments as Natural Sensitizer for TiO₂ Thin Films

Karen Patiño-Camelo,¹ Carlos Diaz-Uribe ,¹ Euler Gallego-Cartagena,² William Vallejo ,¹ Vincent Martinez,¹ Cesar Quiñones,³ Mikel Hurtado,^{4,5} and E. Schott^{6,7}

¹Grupo de Investigación en Fotoquímica y Fotobiología, Programa de Química, Facultad de Ciencias Básicas, Universidad del Atlántico, Carrera 30 # 8-49 Puerto Colombia, Atlántico, Colombia

²Department of Civil and Environmental, Universidad de la Costa, Calle 58 # 55-66, Barranquilla, Colombia

³Institución Universitaria Politécnico Gran Colombiano, Bogotá, Colombia

⁴Departamento de Ingeniería Electrónica, Cluster NBIC, Universidad Central, Bogotá, Colombia

⁵Departamento de Ingeniería Civil, Universidad Minuto de Dios, Bogotá, Colombia

⁶Departamento de Química Inorgánica, Energy Research Center, Facultad de Química, Pontificia Universidad Católica de Chile, Avenida Vicuña Mackenna 4860, Macul, Santiago, Chile

⁷Millennium Nuclei on Catalytic Processes towards Sustainable Chemistry (CSC), Chile

Correspondence should be addressed to Carlos Diaz-Uribe; carlosdiaz@mail.uniatlantico.edu.co

Received 5 April 2019; Revised 21 June 2019; Accepted 10 July 2019; Published 21 August 2019

Academic Editor: Zofia Stasicka

Copyright © 2019 Karen Patiño-Camelo et al. This is an open access article distributed under the Creative Commons Attribution License, which permits unrestricted use, distribution, and reproduction in any medium, provided the original work is properly cited.

In this work, we studied the effect of TiO₂ sensitization with dry biomass extracted of cyanobacteria on the degradation of methylene blue dye (AM). Cyanobacterial cultures isolated from water samples were collected from the swamp of Malambo in Colombia; two main genera of cyanobacteria were identified, and they were cultivated with BG-11 culture medium. The concentrations of *chlorophyll a* in the exponential and stationary phases of growth were measured; the phycobilin content was quantified by spectrophotometry. Thin films of TiO₂ were deposited by a doctor blade method, and they were sensitized by wet impregnation. Furthermore, a methylene blue (MB) photodegradation process was studied under visible light irradiation on the cyanobacterial biomass sensitized TiO₂ material (TiO₂/sensitizer); besides, the pseudo-first-order model was used to obtain kinetic information about photocatalytic degradation. The results showed that the BG-11⁺ treatment reported a higher amount of dry biomass and phycobiliproteins. After the sensitization process, the TiO₂/sensitizer thin films showed a significant red shift in the optical activity; besides the thin film roughness decreasing, the TiO₂/sensitizer showed photocatalytic activity of 23.2% under visible irradiation, and besides, the kinetic (k_{ap}) constant for TiO₂/sensitizer thin films was 3.1 times greater than the k_{ap} value of TiO₂ thin films. Finally, results indicated that cyanobacterial biomass is a suitable source of natural sensitizers to be used in semiconductor sensitization.

1. Introduction

Cyanobacteria are prokaryotic organisms that achieve a high density of biomass, which are increasingly frequent due to the water source eutrophication; this effect is magnified by climate change (e.g., warming and stratification of water, concentration of nutrients); these blooms can generate toxic

secondary metabolites, called cyanotoxins [1, 2]; they can also lead to hypoxia from effluents and disrupt trophic ecosystems [3]. Currently, it represents a serious worldwide environmental problem, due to the fact that harmful cyanobacteria can affect the consumption of drinking water, irrigation, fishing, and recreational waters, which are fundamental for the growing human population [4]. The

Environmental Protection Agency (EPA) of the United States reported that these cyanotoxins can affect human health and other organisms, through dermal exposure, inhalation, and consumption, as it can present bioaccumulation of cyanotoxins in tissues such as the liver in edible fish [5]. Waterbodies are also affected by pollution produced by different industries such as paper mills, textiles, tanneries, and foodstuffs, which use dyes in their processes, which are difficult to be degraded by conventional wastewater treatment technologies [6, 7]. Therefore, wastewater from these industries can create undesirable situations when this waste is generated. Thus, the removal of these types of compounds is extremely important to preserve human health and protect the environment. Several treatment technologies have been used to reduce these pollutants (e.g., coagulation-flocculation, adsorption, chemical precipitation, sedimentation, ion exchange, electrochemistry, and photocatalysis) [8, 9]. Among these methods, heterogeneous photocatalysis allows the generation of reactive oxygen species (ROS); these ROS are extremely reactive, and they can degrade recalcitrant pollutants generated in typical industrial activities. Currently, titanium dioxide (TiO_2) is one of the most studied semiconductors in the field.

However, it is not efficient under visible light, due to its band gap conduction (3.0 to 3.2 eV), which means that only 5% of the total visible light can be used, limiting its applications [10, 11]. Currently, it is necessary to modify the optical constants and the electrical absorption spectrum of TiO_2 into the visible range of the electromagnetic spectrum; these modifications can be achieved through the sensitization of TiO_2 films [12]. A natural or synthetic compound can be used as sensitizers; among these, synthetic dyes are both expensive and harmful to the environment, and besides, natural origin dyes are easier to produce, and they are not harmful to the environment [13].

The pigments of cyanobacteria are of great interest in different industries (e.g., food, textiles, paper, and mill industries), since they are used as natural colorants of their products [14]. In addition to their use as colorants in the food and cosmetic industries, the phycobiliproteins have an interesting application in the advanced oxidation processes in which they are used as sensitizers of TiO_2 ; Kathiravan et al. reported the adsorption of phycocyanin on the surface of colloidal TiO_2 nanoparticles through its carboxylic group [15]; Enciso et al. reported phycocyanin as potential natural dye for its use in photovoltaic cells [16]. Furthermore, the cyanobacterial pigments have been used to improve the photocatalytic TiO_2 activity [17]. However, not much is known about the technological applications of the cyanobacterium consortiums present in aquatic ecosystems, as usually they represent ecological and environmental problems; however, they can be used in the advanced oxidation processes in sensitization of TiO_2 .

In this work, we studied the effect of biomass of cyanobacteria collected from the Malambo swamp of the municipality of Malambo, Department of Atlántico, Colombia, isolated and cultivated in photobioreactors to improve the spectral response of TiO_2 ; this is in order to give a possible biotechnological use to the cyanobacteria that are generating

a problem of environmental contamination in this aquatic ecosystem.

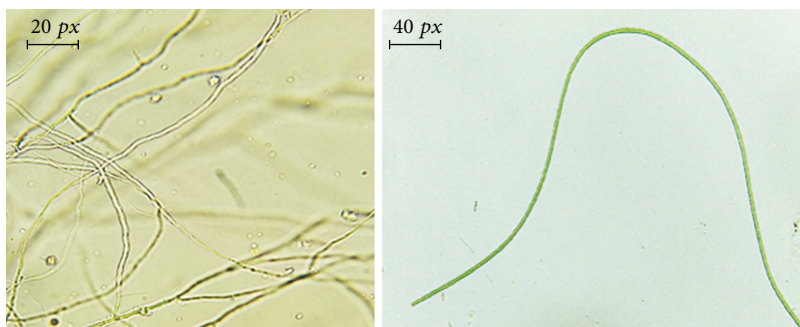
2. Materials and Methods

2.1. Sample Preparation. The samples were obtained from Ciénaga Grande de Malambo, belonging to the Cenagoso Complex of Malambo, located on basin 2904-3, on the left bank of the Magdalena River, located in the Caribbean region of northern Colombia at the geographical coordinates $10^{\circ}85'53''$ north latitude and $74^{\circ}75'64''$ west longitude GPS Garmin Etrex 10. The biological samples were taken in the rainy season of the months of August and September of the year 2017, which are characterized as rainy months with around 14 days/month of rain on average, with average maximum temperature between 31 and 32°C at noon and minimum temperature between 23 and 25°C in the early morning, and with average humidity of 80%. For the collection of samples of cyanobacteria, we used sterilized glass bottles with volumes of 1 liter and a phytoplankton net of 23 μm brand Biologika®. In situ, environmental factors such as salinity and conductivity were determined with the help of a YSI® EcoSense EC300A conductivity meter and water temperature and pH using a YSI® EcoSense 100A pH meter. The samples were stored in a thermoplastic fridge of 30 L capacity.

2.2. Isolation and Identification of Cyanobacterial Strains. We isolated the cyanobacteria using liquid and solid BG-11 medium with an initial pH of 8.3; for that, 200 mL of the water samples was enriched with 50 mL of the liquid BG-11 medium; later, they were taken to the cultivation zone. The solid BG-11 culture medium was used in Petri dishes (3 drops of water in each plate) and incubated at a temperature of $28 \pm 2^{\circ}\text{C}$, with a photoperiod of 8 days of light and 16 hours of dark exposure. The incubation time was approximately 3 weeks; the incubation was carried out in the culture area which consisted of a discontinuous culture system, composed of fluorescent tube lamps 21 W (6400 K of 1700 lm), Deko-Light brand ($21.4 \mu\text{mol m}^{-2} \text{s}^{-1}$), and controlled temperature of $26 \pm 2^{\circ}\text{C}$ [18]. The taxonomic identification of the genus was made at the microscopic level with the help of a Leica DM 500 optical microscope with a Leica ICC50 HD built-in camera. For identification, taxonomic keys of Komárek [19], Anagnostidis and Komárek [20], Cirés and Quesada [21], and AlgaeBase [22] information were used. The morphological characteristics of the isolates considered for taxonomic identification were the following: formation of colonies and filaments, thickness of the filament, shape and size of intercalary cells and filament terminals, presence of necridial cells, presence or absence of constrictions in the crossing of the wall, number of trichomes per filament, absence or presence and color of the pod, and presence and shape of the heterozygotes.

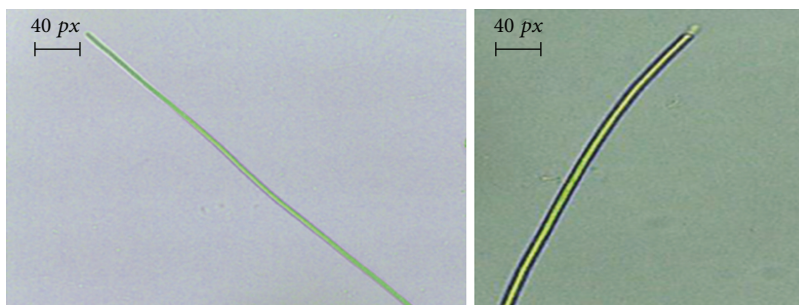
2.3. Photosynthetic Pigment Quantification. We studied the nitrate variation of the BG-11 culture medium on the behavior of the biomass of the cyanobacteria. The control was taken (BG-11 medium with 1.50 g of NaNO_3); the first variation is BG-11₀ (BG-11 without NaNO_3), and the second

Super kingdom: Prokaryotae
 Kingdom: Eubacteria
 Subkingdom: Negibacteria
 Phylum: Cyanobacteria
 Class: Cyanophyceae
 Subclass: Synechococcophycidae
 Order: Synechococcales
 Family: Leptolyngbyaceae
 Genus: *Leptolyngbya*



(a)

Super kingdom: Prokaryotae
 Kingdom: Eubacteria
 Subkingdom: Negibacteria
 Phylum: Cyanobacteria
 Class: Cyanophyceae
 Subclass: Oscillatoriophycidae
 Order: Oscillatoriales
 Family: Oscillatoriaceae
 Genus: *Lyngbya*



(b)

FIGURE 1: Taxonomic classification of cyanobacteria in the water samples: (a) *Leptolyngbya* and (b) *Lyngbya* [19–22].

variation is BG-11⁺ (BG-11 with 3.00 g of NaNO₃). The main pigments of the cyanobacteria were determined such as *chlorophyll a* and *phycobiliproteins* during the phases of exponential growth (day 12) and stationary (day 24). The concentration of *chlorophyll a* was calculated according to the equations of Jeffrey and Humphrey methodology, and the concentration of the pigments of *phycocyanin-C* (C-PC) and *allophycocyanin* (APC) was calculated according to the Fernández et al. equations [23].

2.4. TiO₂ Thin Film Fabrication. The use of thin films of TiO₂ in the treatment of water prevents agglomeration and leaching of nanoparticles during the operation of the catalysis, solving one drawback of the photocatalysis in powder suspensions associated with the recovery of the TiO₂ nanoparticles after the treatment process [24]. TiO₂ powder (P25) was purchased from Merck, with a mean particle size of ~25 nm TiO₂; details of slurry preparation are reported in [10, 25]. Thin films were deposited by using the doctor blade method on soda lime glass substrates. The obtained TiO₂ thin films were dried for 15 min on a hot plate at 100°C. Finally, they were annealed at 450°C for 1 hour.

2.5. TiO₂ Thin Film Sensitization and Characterization. In the sensitization process, dried biomass (40 and 80 mg) was weighed, and 50 mL of distilled water was added to prepare dissolved concentrations of 800 and 1600 ppm, respectively. The TiO₂ films obtained were submerged in the dilutions in 1 L for 12 hours in constant agitation in a magnetic stirrer brand Velp Scientifica Multistirrer at room temperature. After that, the films were dried at room temperature and in darkness, for which they were deposited in boxes of Petri lined with craft paper to protect them from light. To verify

the change of the photoresponse of sensitized TiO₂ films in the visible range of the electromagnetic spectrum, a diffuse reflectance spectrophotometry analysis was performed using a Beijing Elmer Lambda 4 spectrometer equipped with an integrating sphere. The surface morphology of as-grown TiO₂ and sensitized TiO₂ thin films was studied using a Cypher ES (Asylum Research) Microscope, atomic force microscopy (AFM) with a scanned area (10 μm × 10 μm) in a tapping mode. Finally, film thickness was measured using a Veeco Dektak 150 profilometer.

2.6. Photocatalytic Test. The photodegradation experiment was carried out using a batch-type photoreactor with Opalux 8 W 2500 K Blue 45% lamps. All the photodegradation tests were carried out with a volume of 50 mL of an aqueous solution of methylene blue labeled at 2.0 and 4.0 ppm. The films were immersed in the solution and placed inside the photoreactor. Prior to irradiation, the solution was stirred for 30 minutes in the dark in order to ensure that the adsorption/desorption equilibrium of the pollutant was reached. During the irradiation test, the solution was stirred constantly for 140 minutes; the MB concentration was determined by using absorbance at 664 nm in a Hach DR 3800 spectrophotometer.

3. Results and Discussion

3.1. Taxonomic Identification. We identified taxonomically 2 genera of cyanobacteria in the water samples collected from the Malambo swamp. We identified the genera *Raphidiopsis* [26] and *Lyngbya* [27] which are described in detail in Figure 1.

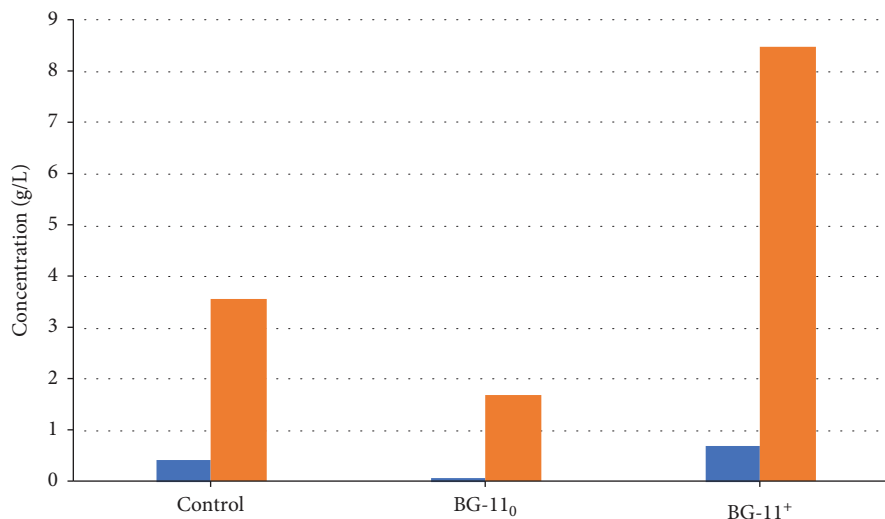


FIGURE 2: Growth cyanobacteria biomass for different contents of NaNO_3 at the BG-11 culture medium.

TABLE 1: Chlorophyll quantification for different biomass growing stages.

Stage	Chlorophyll a ($\mu\text{g}/\text{mL}$)	Percentage (%)
Exponential	0.057	0.0019
Stationary	0.156	0.0052
Dry biomass	0.463	0.0154

3.2. Chlorophyll and Phycobiliprotein Quantification. The growth of cyanobacterial biomass was followed by the weight in grams. Figure 2 shows the results obtained for the exponential phase at 12 days of culture and the stationary phase at 24 days of culture for the three levels of study of nutrient content. The results show least representative content values for BG-11₀ treatment, the absence of the nutrient NaNO_3 ; during the whole trial, the presence of the genus of cyanobacteria *Lyngbya*, *Arthrospira*, and *Microcystis* was observed which lack the presence of heterocysts, organelles used by these microorganisms in the synthesis of atmospheric nitrogen, so they need this nutrient for their metabolic functions; higher content of cyanobacteria biomass was observed in the treatment BG-11⁺.

Table 1 describes the values and percentages for the initial, exponential, and stationary phases of biomass growing. Table 1 also listed the concentrations obtained after drying the biomass.

The results obtained for the chlorophyll a quantification indicate a higher concentration value during the stationary phase of the assay with $0.156 \mu\text{g}/\text{mL}$, which agrees with other investigations that have determined that the production of chlorophyll is higher in this phase for some cultivated microalgae with BG-11 medium [28]. On the other hand, $0.463 \mu\text{g}/\text{mL}$ was obtained in the extraction of the pigment in the dry biomass, which corresponds to 0.0154% of the total volume of the sample used for the analysis; this could have been presented since in the drying process this pigment

became hyperconcentrated. Table 2 shows the results of the quantification of the phycobiliproteins (phycocyanins-C and allophycocyanins) from the biomass of cyanobacteria in the initial phase and besides, before and after drying the biomass.

The highest values were obtained for the BG-11⁺ treatment with $1021.0 \mu\text{g}/\text{mL}$. In addition, we observed that the concentration values of phycobilins after drying the biomass were slightly lower, maybe because during the drying process these pigments could have been denatured as they are water-soluble pigments.

3.3. TiO_2 /Sensitized Thin Film Optical Characterization.

After pigment quantification, we proceed to determine the effect of the sensitization process on thin film properties; the optical characterization was carried out to determine sensitization effect on semiconductor behavior. The optical properties of TiO_2 /sensitizer thin films were determined from diffuse reflectance measurements between the range of 400 and 800 nm. Figure 3 shows the diffuse reflectance spectrum of TiO_2 films sensitized with dry biomass of cyanobacteria after 12 hours of sensitization with two sensitizer concentrations of 800 ppm and 1600 ppm. Figure 3 shows that the TiO_2 films did not show optical activity at a visible range of the electromagnetic spectrum; this result is typical of TiO_2 due to its band gap value (3.20 eV, see Table 3); in comparison, for TiO_2 thin films sensitized with dry biomass of cyanobacteria, two shoulders located at approximately 660 and 460 nm are observed; this result is relevant and indicates that the sensitization process was carried out and that the fabricated electrode is active in the visible range of the spectrum.

The shoulders observed inside of the reflectance spectrum indicate that the TiO_2 /sensitizer thin films are optically active in the visible region of electromagnetic spectrum; in the sensitization process, the sensitizer alters the semiconductor by two ways: (a) energy transfer and (b) electronic

TABLE 2: Phycobiliprotein quantification in different growth stages.

Phase	Phycocyanin-C		Phycobiliproteins ($\mu\text{g}/\text{mL}$) Allophycocyanin		Total	
	Value	Percentage	Value	Percentage	Value	Percentage
Control	703.5	0.014	272.8	0.005	976.3	0.019
BG-11 ₀	656.1	0.013	266.2	0.005	922.3	0.018
BG-11 ⁺	736.2	0.015	284.8	0.005	1021.0	0.020
Dry biomass	568.9	0.012	182.9	0.003	751.8	0.015

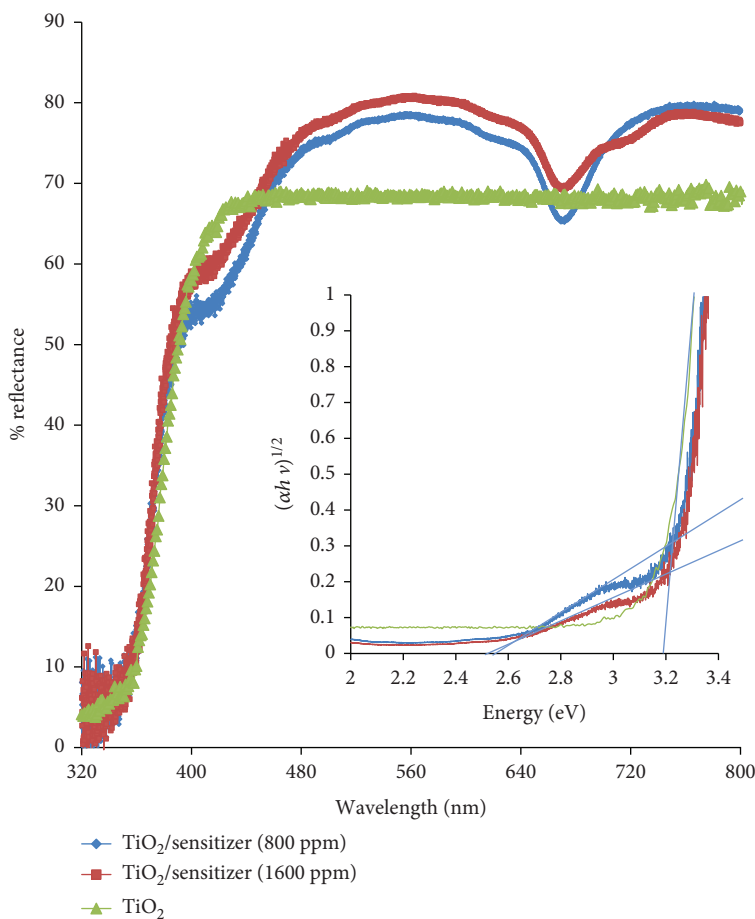


FIGURE 3: Diffuse reflectance spectrum of $\text{TiO}_2/\text{sensitizer}$ using two loads of cyanobacterial biomass; inset: it is showing the analog to Tauc plots for reflectance spectra.

TABLE 3: The energy band gap values for thin films.

Thin film	Band gap composites (eV)
TiO_2	3.20
$\text{TiO}_2/\text{sensitizer}$ (800 ppm)	2.55
$\text{TiO}_2/\text{sensitizer}$ (1600 ppm)	2.55

transfer from sensitizer to semiconductor after radiation absorption [29]; Figure 3 shows typical signals for phycocyanins (phycocyanin-C and allophycocyanin), with a maximum spectral profile of 615, 340, and 260 and shoulders at 650 and 400 nm. These results agree with other reports;

Xiang et al. reported that sensitizer can anchor to the TiO_2 surface as $\text{Ti-O-CH}_2\text{-OH}$ on the TiO_2 surface by thermal treatment, which allows TiO_2 to have a greater capacity for light capture and efficient electron transport [17]; Phongamwong et al. reported similar behavior [30].

Theoretical reports on anthocyanin adsorption on TiO_2 indicated that hydroxyl groups can act as a bridge for bonding semiconductor and natural sensitizer [10]. In the work presented here, it is possible that the carboxyl groups available in the phycocyanin structure can be responsible for anchoring to the TiO_2 surface during the sensitization process; Figure 4 shows the general scheme of the hypothetical sensitization process. Enciso et al. reported phycocyanin

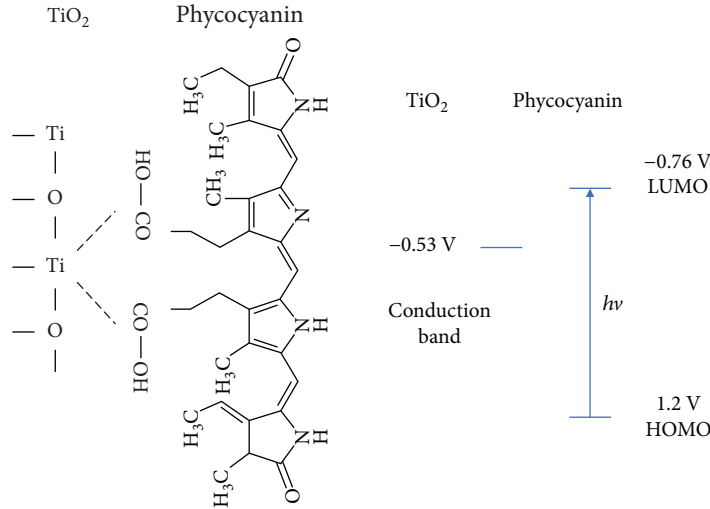


FIGURE 4: Hypothetical sensitization process and energy levels for phycocyanin sensitization [31, 32].

sensitization of TiO_2 for DSSC applications; in that work, they reported the energy levels for system $\text{TiO}_2/\text{phycocyanin}$ (Figure 4); according to this report, phycocyanins have the lowest unoccupied molecular orbital (LUMO) energy higher (-0.76 V) than the value for the conduction potential of TiO_2 (0.53 V). In this sense, after the sensitization process, phycocyanins absorb visible light, and according to oxidation potential, it is possible to predict a spontaneous process of electron transference between phycocyanins and TiO_2 [32]; this implies that the $\text{TiO}_2/\text{phycocyanin}$ system should be photocatalytic active into a visible electromagnetic spectrum; this is studied in Section 3.4.

The band gap energy value was determined for all samples using the Kubelka-Munk remission function [33, 34]:

$$\frac{k}{s} = F(R_\infty) = \frac{(1 - R_\infty)^2}{2R_\infty}, \quad (1)$$

where R_∞ is the material reflectance value and $F(R_\infty)$ represents the ratio between the absorption and the scattering coefficients (k/s); $F(R_\infty)$ is proportional to the constant of absorption of the material, an indication of the sample absorbance at a particular wavelength. From equation (1) and the curves shown in Figure 3, an analog to Tauc plots ($F(R_\infty) \cdot hv$)^{1/2} against photon energy can be constructed, according to [34–36]:

$$(F(R_\infty)hv)^{1/2} = A(hv - E_g). \quad (2)$$

Inside Figure 3, we show the relationship between $(ahv)^{1/2}$ and the photonic energy for the diffuse reflectance; the value of the band gap of the films was determined by extrapolating the linear portion of the graph on the x -axis [37]. Table 3 listed the optical properties of $\text{TiO}_2/\text{sensitizers}$.

3.4. $\text{TiO}_2/\text{Sensitized Thin Film Morphological Characterization}$. Figure 5 shows AFM images for TiO_2 and $\text{TiO}_2/\text{sensitized thin films}$. Results show that TiO_2 films are

composed of aggregates with size in a range around 150 nm - 170 nm . Figure 5 shows that morphology of the TiO_2 surface (grain size and roughness) is affected by the sensitization process. Table 4 shows that the roughness of the TiO_2 film is greater than the roughness of the sensitized films; this occurs because, during the first stage of the process, the sensitizer occupies the free spaces on the surface of TiO_2 (spaces with greater surface energy) which caused the roughness to decrease [38].

These results indicate that after the sensitization process, the electrodes were more uniform. Table 4 shows the roughness and grain size values of the films obtained for the synthesized films.

3.5. Photocatalytic Test. Figure 6 shows the behavior for all the tests; unmodified TiO_2 thin films did not show significant degradation yield under visible irradiation; this is a typical behavior for TiO_2 due to their well-known wide band gap value. Results for the experiments with $\text{TiO}_2/\text{sensitizer thin films}$ showed an important increase in the photocatalytic response in the visible range of the electromagnetic spectrum, and a photodegradation of 24.3% ($\text{TiO}_2/\text{sensitizer } 800\text{ ppm}$) and 25.3% ($\text{TiO}_2/\text{sensitizer } 1600\text{ ppm}$) was achieved after 140 min of irradiation. Results show that most higher dye concentration reduction was due to the presence of natural sensitizer. A pseudo-first-order model was applied to kinetic data of Figure 5(a) [39]:

$$C_t = C_0 e^{-k_{ap} \cdot t}, \quad (3)$$

where the unit of time (t) is minutes, k_{ap} is the apparent reaction rate constant (min^{-1}), and C_t is the concentration of MB as a function of time.

The k_{ap} values for each test were determined from the slope of the linear fitting of Figure 5(b). Both thin films $\text{TiO}_2/\text{sensitizer } (800\text{ ppm})$ and $\text{TiO}_2/\text{sensitizer } (1600\text{ ppm})$ had the same k_{ap} value ($1.6 \times 10^{-3}\text{ min}^{-1}$); results did not show significant difference for k_{ap} values; in this case, the

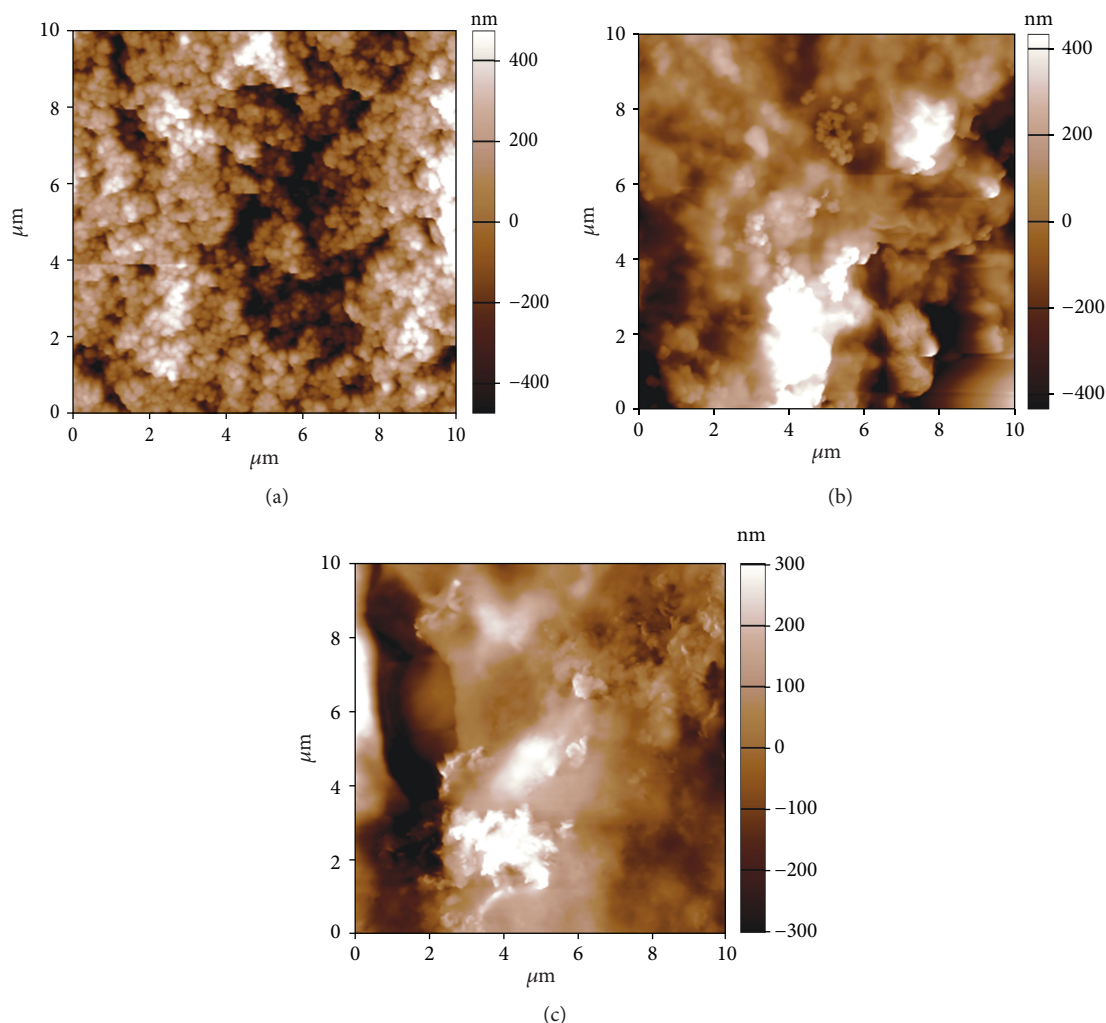


FIGURE 5: AFM images of (a) TiO_2 , (b) $\text{TiO}_2/\text{sensitizer}$ (800 ppm), and (c) $\text{TiO}_2/\text{sensitizer}$ (1600 ppm) thin films.

TABLE 4: Roughness and grain size of TiO_2 and $\text{TiO}_2/\text{sensitizer}$ thin films.

Thin films	Grain size (nm)	Roughness (nm)
TiO_2	170	75
$\text{TiO}_2/\text{sensitizer}$ (800 ppm)	174	65
$\text{TiO}_2/\text{sensitizer}$ (1600 ppm)	150	49

concentration of sensitizer in the solution used during the sensitization process has the same effect. After 12 hours of sensitization, both the initial sensitizer concentrations (800 ppm and 1600 ppm) have the same effect; this result is according to optical results; band gap was the same for both samples. The k_{ap} value for $\text{TiO}_2/\text{sensitizer}$ thin films was 3.1 times greater than the k_{ap} value ($5.0 \times 10^{-4} \text{ min}^{-1}$) of TiO_2 thin films.

Other reports related to the surface engineering of photocatalysts take advantage of physical-chemical synthesis parameters to enhance visible light photocatalytic performances; Siyuan et al. reported the NaBH_4 reduction method

to engineer the surface of flake-like Bi_2WO_6 [40], and Zhao et al. reported the NaBH_4 reduction method to create surface disorder on $\text{Bi}_4\text{Ti}_3\text{O}_{12}$ nanosheets [41]. In both cases, photocatalytic activities were improved after the modification process; in our case, the sensitization process was achieved from a natural source reducing costs and environmental impact. The results indicate that the sensitization process was effective and demonstrated that cyanobacterial biomass can act as an alternative sensitizer of TiO_2 . Finally, this potential application becomes an alternative solution to the continuous growth of cyanobacterial biomass in the swamps.

4. Conclusions

The pigment values extracted were higher when biomass was dried ($0.463 \mu\text{g}/\text{mL}$ of chlorophyll a) at a volume of analysis of 3 mL. For the phycocyanins, the highest content value was obtained for BG-11⁺ treatment. The diffuse reflectance verified that the biomass adhered to the TiO_2 surface; after the sensitization process, thin films showed a redshift band gap

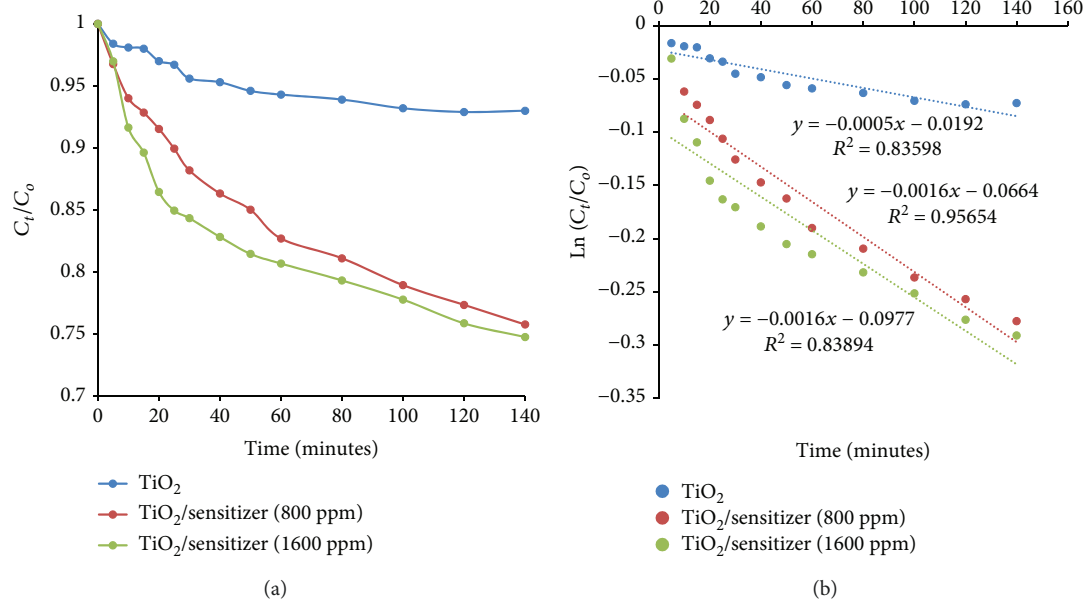


FIGURE 6: (a) MB degradation under visible irradiation. (b) Linear fitting $\ln(C_t/C_0)$ vs. (t) for test. C_t refers to concentration at time t of MB, and C_0 refers to initial concentration.

from 3.20 eV to 2.55 eV; the morphological results showed that films were composed of aggregates with size in a range around 150 nm-170 nm. After the sensitization process, the degradation tests showed 25.3% of degradation under visible irradiation. Finally, results indicated that natural extract obtained from cyanobacterial biomass has suitable properties to be used in TiO_2 sensitization.

Data Availability

The data used to support the findings of this study are available from the corresponding author upon request.

Conflicts of Interest

The authors declare that they have no conflicts of interest.

Acknowledgments

C.D.-U. and W.V. thank Universidad del Atlántico (Project Code CB23-TGI2018). E.G.C. thanks Centro de Investigaciones de Tecnologías Ambientales at Universidad de la Costa. E.S.V. thanks FONDECYT 1161416, SERC FONDAP 15110019, and Millennium Science Initiative of the Ministerio de Economía, Fomento y Turismo, Chile, grant Nuclei on Catalytic Processes towards Sustainable Chemistry (CSC). This work was supported by Universidad del Atlántico and Universidad de la Costa.

References

- [1] G. S. Bullerjahn, R. M. McKay, T. W. Davis et al., "Global solutions to regional problems: collecting global expertise to address the problem of harmful cyanobacterial blooms. A Lake Erie case study," *Harmful Algae*, vol. 54, pp. 223–238, 2016.
- [2] E. Funari, M. Manganelli, F. M. Buratti, and E. Testai, "Cyanobacteria blooms in water: Italian guidelines to assess and manage the risk associated to bathing and recreational activities," *Science of the Total Environment*, vol. 598, pp. 867–880, 2017.
- [3] H. W. Paerl, W. S. Gardner, K. E. Havens et al., "Mitigating cyanobacterial harmful algal blooms in aquatic ecosystems impacted by climate change and anthropogenic nutrients," *Harmful Algae*, vol. 54, pp. 213–222, 2016.
- [4] P. M. Visser, J. M. H. Verspagen, G. Sandrini et al., "How rising CO_2 and global warming may stimulate harmful cyanobacterial blooms," *Harmful Algae*, vol. 54, pp. 145–159, 2016.
- [5] Environmental Protection Agency, *Cyanobacteria and cyanotoxins: information for drinking water systems*, pp. 1–11, 2014, https://www.epa.gov/cyanobacteria_factsheet.pdf.
- [6] R. Dewil, D. Mantzavinos, I. Poullos, and M. A. Rodrigo, "New perspectives for advanced oxidation processes," *Journal of Environmental Management*, vol. 195, Part 2, pp. 93–99, 2017.
- [7] V. Gitis and N. Hankins, "Water treatment chemicals: trends and challenges," *Journal of Water Process Engineering*, vol. 25, pp. 34–38, 2018.
- [8] L. Wolski and M. Ziolk, "Insight into pathways of methylene blue degradation with H_2O_2 over mono and bimetallic Nb, Zn oxides," *Applied Catalysis B: Environmental*, vol. 224, pp. 634–647, 2018.
- [9] D. Pathania, S. Sharma, and P. Singh, "Removal of methylene blue by adsorption onto activated carbon developed from *Ficus carica* bast," *Arabian Journal of Chemistry*, vol. 10, pp. S1445–S1451, 2017.
- [10] C. Díaz-Urbe, W. Vallejo, K. Campos et al., "Improvement of the photocatalytic activity of TiO_2 using Colombian Caribbean species (*Syzygium cumini*) as natural sensitizers: experimental and theoretical studies," *Dyes and Pigments*, vol. 150, pp. 370–376, 2018.
- [11] D. Liu, R. Tian, J. Wang et al., "Photoelectrocatalytic degradation of methylene blue using F doped TiO_2 photoelectrode

- under visible light irradiation,” *Chemosphere*, vol. 185, pp. 574–581, 2017.
- [12] W. Vallejo, C. Diaz-Urbe, and Á. Cantillo, “Methylene blue photocatalytic degradation under visible irradiation on TiO₂ thin films sensitized with Cu and Zn tetracarboxyphthalocyanines,” *Journal of Photochemistry and Photobiology A: Chemistry*, vol. 299, pp. 80–86, 2015.
- [13] M. A. M. Al-Alwani, A. B. Mohamad, A. A. H. Kadhum, and N. A. Ludin, “Effect of solvents on the extraction of natural pigments and adsorption onto TiO₂ for dye-sensitized solar cell applications,” *Spectrochimica Acta Part A: Molecular and Biomolecular Spectroscopy*, vol. 138, pp. 130–137, 2015.
- [14] N.-S. Lau, M. Matsui, and A. A. A. Abdullah, “Cyanobacteria: photoautotrophic microbial factories for the sustainable synthesis of industrial products,” *BioMed Research International*, vol. 2015, Article ID 754934, 9 pages, 2015.
- [15] A. Kathiravan, M. Chandramohan, R. Renganathan, and S. Sekar, “Cyanobacterial chlorophyll as a sensitizer for colloidal TiO₂,” *Spectrochimica Acta Part A: Molecular and Biomolecular Spectroscopy*, vol. 71, no. 5, pp. 1783–1787, 2009.
- [16] P. Enciso, M. Cabrerizo, J. Gancheff, P. Denis, and M. Cerda, “Phycocyanin assemblies onto nanostructured TiO₂ for photovoltaic cells,” *Journal of Applied Solution Chemistry and Modeling*, vol. 2, pp. 225–233, 2013.
- [17] C. Xiang, C. A. Okonkwo, Q. Xiong, L. Wang, and L. Jia, “A novel TiO₂ film photoanode decorated with spirulina-derived residual groups for enhanced photocurrent in dye-sensitized solar cells,” *Solar Energy*, vol. 134, pp. 461–467, 2016.
- [18] R. S. Gour, M. Bairagi, V. K. Garlapati, and A. Kant, “Enhanced microalgal lipid production with media engineering of potassium nitrate as a nitrogen source,” *Bioengineered*, vol. 9, no. 1, pp. 98–107, 2018.
- [19] J. Komárek, J. Kaštoký, J. Mareš, and J. R. Johansen, “Taxonomic classification of cyanoprokaryotes (cyanobacterial genera) 2014, using a polyphasic approach,” *Preslia*, vol. 86, pp. 295–335, 2014.
- [20] K. Anagnostidis and J. Komárek, “Modern approach to the classification system of the cyanophytes. 3-Oscillatoriales,” *Algalological Studies*, vol. 50–53, pp. 327–472, 1988.
- [21] S. Cirés and A. Quesada, *Catálogo de cianobacterias planctónicas potencialmente tóxicas de las aguas continentales españolas*, Ministerio de Medio Ambiente y Medio Rural y Marino, 2011.
- [22] AlgaeBase, “M.D. Guiry,” 2019, <http://www.algaebase.org/>.
- [23] J. A. Fernández, A. Suan, J. C. Ramírez et al., “Treatment of real wastewater with TiO₂-films sensitized by a natural-dye obtained from *Picramnia sellowii*,” *Journal of Environmental Chemical Engineering*, vol. 4, no. 3, pp. 2848–2856, 2016.
- [24] E. Rice, R. Baird, A. Eaton, and L. Clescerl, *Standard Methods for Examination of Water and Wastewater*, American Public Health Association, Washington DC, USA, 22a edition, 2012.
- [25] C. Quiñones, Y. Ayala, and W. Vallejo, “Methylene blue photoelectrodegradation under UV irradiation on Au/Pd-modified TiO₂ films,” *Applied Surface Science*, vol. 257, no. 2, pp. 367–371, 2010.
- [26] F. E. Fritsch and F. Rich, “Freshwater algae from Griqualand West,” *Transactions of the Royal Society of South Africa*, vol. 18, no. 1, pp. 1–92, 1929.
- [27] M. Gomont, “Monographie des Oscillariées (Nostocacées Homocystées). Deuxième partie. - Lyngbyées,” *Annales des sciences Naturelles, Botanique, Série*, vol. 7, no. 16, pp. 91–264, 1892, pls 1-7.
- [28] M. Hamadani, J. Safaei-Ghomi, M. Hosseinpour, R. Masoomi, and V. Jabbari, “Uses of new natural dye photosensitizers in fabrication of high potential dye-sensitized solar cells (DSSCs),” *Materials Science in Semiconductor Processing*, vol. 27, pp. 733–739, 2014.
- [29] Ü. İsci, M. Beyreis, N. Tortik et al., “Methylsulfonyl Zn phthalocyanine: a polyvalent and powerful hydrophobic photosensitizer with a wide spectrum of photodynamic applications,” *Photodiagnosis and Photodynamic Therapy*, vol. 13, pp. 40–47, 2016.
- [30] T. Phongamwong, M. Chareonpanich, and J. Limtrakul, “Role of chlorophyll in spirulina on photocatalytic activity of CO₂ reduction under visible light over modified N-doped TiO₂ photocatalysts,” *Applied Catalysis B: Environmental*, vol. 168–169, pp. 114–124, 2015.
- [31] J. Lim, A. D. Bokare, and W. Choi, “Visible light sensitization of TiO₂ nanoparticles by a dietary pigment, curcumin, for environmental photochemical transformations,” *RSC Advances*, vol. 7, no. 52, pp. 32488–32495, 2017.
- [32] P. Enciso, F. M. Cabrerizo, J. S. Gancheff, P. A. Denis, and M. F. Cerdá, “Phycocyanin as potential natural dye for its use in photovoltaic cells,” *Journal of Applied Solution Chemistry and Modeling*, vol. 2, pp. 225–233, 2013.
- [33] E. L. Simmons, “Relation of the diffuse reflectance remission function to the fundamental optical parameters,” *Optica Acta: International Journal of Optics*, vol. 19, no. 10, pp. 845–851, 1972.
- [34] J. Tauc, R. Grigorovici, and A. Vancu, “Optical properties and electronic structure of amorphous germanium,” *Physica Status Solidi (b)*, vol. 15, no. 2, pp. 627–637, 1966.
- [35] B. D. Viezbicke, S. Patel, B. E. Davis, and D. P. Birnie III, “Evaluation of the Tauc method for optical absorption edge determination: ZnO thin films as a model system,” *Physica Status Solidi (b)*, vol. 252, no. 8, pp. 1700–1710, 2015.
- [36] W. Vallejo, A. Rueda, C. Díaz-Urbe, C. Grande, and P. Quintana, “Photocatalytic activity of graphene oxide–TiO₂ thin films sensitized by natural dyes extracted from *Bactris guineensis*,” *Royal Society Open Science*, vol. 6, no. 3, article 181824, 2019.
- [37] S. Khaleghi, “Calculation of electronic and optical properties of doped titanium dioxide nanostructure,” *Journal of Nanostructures*, vol. 2, no. 2, pp. 157–161, 2012.
- [38] T. S. Senthil, N. Muthukumarasamy, S. Agilan, R. Balasundaraprabhu, and C. K. Senthil Kumaran, “Effect of surface morphology on the performance of natural dye sensitized TiO₂ thin film solar cell,” *Advanced Materials Research*, vol. 678, pp. 326–330, 2013.
- [39] I. K. Konstantinou and T. A. Albanis, “TiO₂-assisted photocatalytic degradation of azo dyes in aqueous solution: kinetic and mechanistic investigations: a review,” *Applied Catalysis B: Environmental*, vol. 49, no. 1, pp. 1–14, 2004.
- [40] S. Wang, H. Yang, X. Wang, and W. Feng, “Surface disorder engineering of flake-like Bi₂WO₆ crystals for enhanced photocatalytic activity,” *Journal of Electronic Materials*, vol. 48, no. 4, pp. 2067–2076, 2019.
- [41] X. Zhao, H. Yang, H. Zhang, Z. Cui, and W. Feng, “Surface-disorder-engineering-induced enhancement in the photocatalytic activity of Bi₄Ti₃O₁₂ nanosheets,” *Desalination and Water Treatment*, vol. 145, pp. 326–336, 2019.

